iScience

CellPress
OPEN ACCESS

Article

Islet-resident macrophage-derived miR-155 promotes β cell decompensation via targeting PDX1

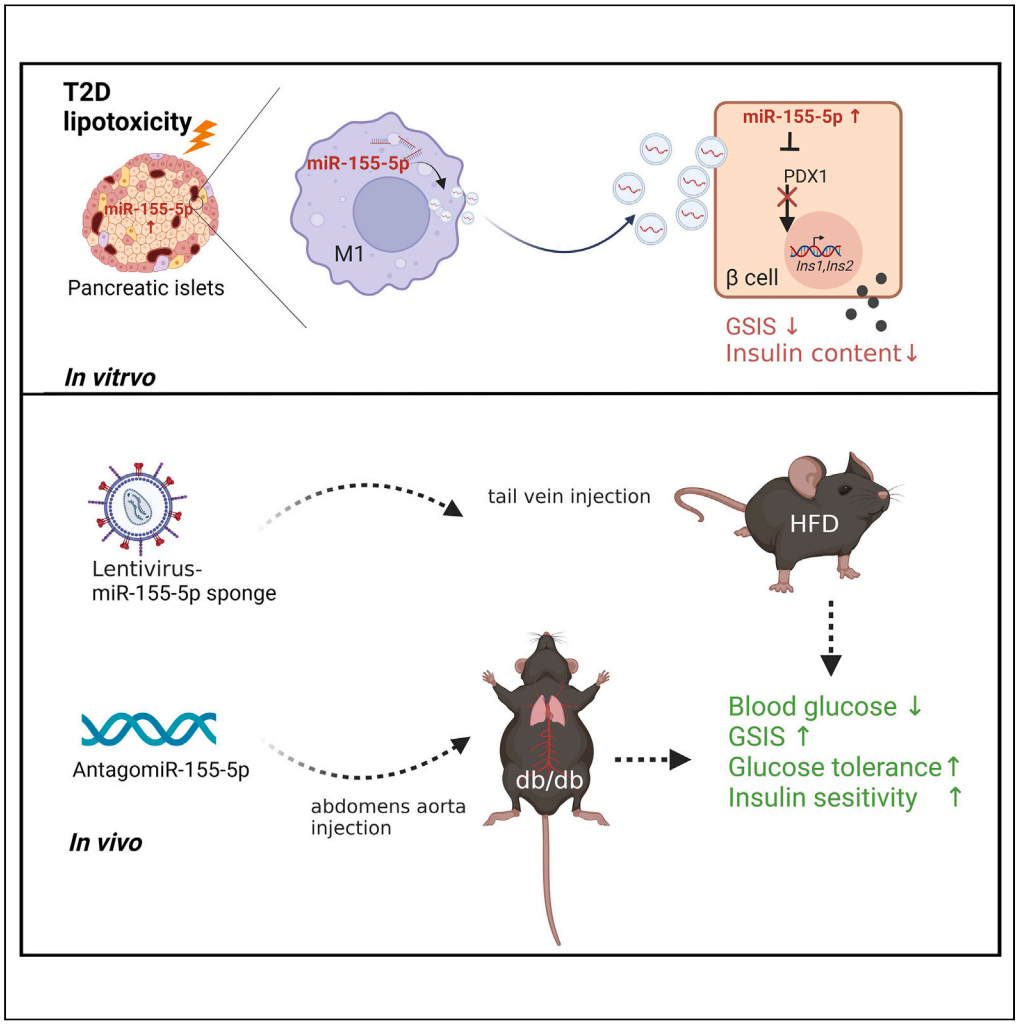

Yan Zhang, Rong Cong, Tingting Lv, ..., Yating Li, Xiao Han, Yunxia Zhu

zhuyx@njmu.edu.cn

Highlights

miR-155 is elevated in type-2 diabetic islets due to islet-resident macrophages

Inhibiting miR-155 improves β cell function to ease inflammation-linked diabetes

Macrophage-derived exosomal miR-155 disrupts β cell function by targeting PDX1

Blocking macrophage miR-155 or reconstituting β cell PDX1 rescues insulin secretion

Zhang et al., iScience 27, 109540
April 19, 2024
https://doi.org/10.1016/j.isci.2024.109540

iScience

CellPress
OPEN ACCESS

Article

Islet-resident macrophage-derived miR-155 promotes β cell decompensation via targeting PDX1

Yan Zhang,[1,2] Rong Cong,[1,2] Tingting Lv,[1,2] Kerong Liu,[1] Xiaoai Chang,[1] Yating Li,[1] Xiao Han,[1] and Yunxia Zhu[1,3,*]

SUMMARY

Chronic inflammation is critical for the initiation and progression of type 2 diabetes mellitus via causing both insulin resistance and pancreatic β cell dysfunction. miR-155, highly expressed in macrophages, is a master regulator of chronic inflammation. Here we show that blocking a macrophage-derived exosomal miR-155 (MDE-miR-155) mitigates the insulin resistances and glucose intolerances in high-fat-diet (HFD) feeding and type-2 diabetic db/db mice. Lentivirus-based miR-155 sponge decreases the level of miR-155 in the pancreas and improves glucose-stimulated insulin secretion (GSIS) ability of β cells, thus leading to improvements of insulin sensitivities in the liver and adipose tissues. Mechanistically, miR-155 increases its expression in HFD and db/db islets and is released as exosomes by islet-resident macrophages under metabolic stressed conditions. MDE-miR-155 enters β cells and causes defects in GSIS function and insulin biosynthesis via the miR-155-PDX1 axis. Our findings offer a treatment strategy for inflammation-associated diabetes via targeting miR-155.

INTRODUCTION

Type 2 diabetes mellitus (T2D) is a metabolic syndrome characterized by insulin resistance and pancreatic β cell dysfunction.[1–3] Although the pathogenesis of T2D remains obscure, β cell dysfunction is a recognized major cause of T2D.[4,5] Increasing evidence now shows that insulitis, dominated by macrophage infiltration, is observed in the pancreatic islets of T2D patients,[6–10] suggesting inflammatory microenvironment of islet may play key roles in promoting β cell dysfunction. Macrophages are ubiquitous in tissues and exhibit polarized M1 or M1 phenotypes.[11–14] During pre-diabetic period, intra-islet M1 macrophage infiltration has been noted to initiate insulitis, impair β cell insulin secretion, and contribute to a higher susceptibility to T2D in obese individuals,[15–17] which indicates that suppressing intra-islet inflammation in the early stage of T2D is vital for protecting β cell function from disruption by macrophages.[11,18] Therefore, revealing the crosstalk between macrophage and β cell dysfunction will provide potent evidence for anti-inflammatory therapy of T2D.

Multiple lines of evidence have shown that the infiltration of macrophages in islets disturbs β cell insulin secretion and induces β cell apoptosis by secreting large amounts of several inflammatory factors.[13,19] Intriguingly, emerging evidence now indicates that macrophages can secrete microRNA (miRNA)-rich exosomes to target cells,[20,21] suggesting that this type of secretion might mediate inflammation-induced β cell dysfunction in T2D. Considerable research has demonstrated high expression of miR-155 in M1 macrophages isolated from adipose tissues from obese individuals (adipose tissue macrophages; ATMs)[20,22,23] and that the secretion of miR-155 into peripheral circulation in exosomes causes glucose intolerance and insulin resistance.[23] Notably, T2D patients show clear dysregulation of serum miR-155 expression.[24] Moreover, inhibition of miR-155 can mitigate diabetic complications by accelerating diabetic wound healing,[25] alleviating diabetic acute kidney injury,[26] and protecting against diabetic osteoporosis,[27] indicating the potential involvement of miR-155 in the development of T2D. Interestingly, Regazzi et al. have demonstrated that miR-155 derived from lymphocyte of islets promoted β cell death and contributes to type 1 diabetes (T1D) development in non-obese diabetic (NOD) mice.[28] Nevertheless, it remains unclear whether miR-155 in type-2 diabetic islets mediates the crosstalk between macrophages and β cells to participate in the development of T2D.

In this study, we observed the expression of miR-155 was elevated in islets of T2D mice that derived from islet-resident M1 macrophages (MDE-miR-155). MDE-miR-155 entered β cells via exosomes to cause β cell dysfunction by targeting PDX1. *In vivo*, we demonstrated that inhibition of miR-155 improved T2D symptoms by increasing β cell insulin secretion and mitigating insulin resistance in high-fat-diet (HFD)-fed and db/db diabetic mice. Therefore, our findings revealed that miR-155 mimicked inflammation-induced β cell dysfunction in T2D while its inhibition exerted obvious therapeutic effect, suggesting that targeting miR-155 may be a promising treatment strategy for T2D.

[1]Key Laboratory of Human Functional Genomics of Jiangsu Province, Department of Biochemistry and Molecular Biology, Nanjing medical University, Nanjing, Jiangsu 211166, China
[2]These authors contributed equally
[3]Lead contact
*Correspondence: zhuyx@njmu.edu.cn
https://doi.org/10.1016/j.isci.2024.109540

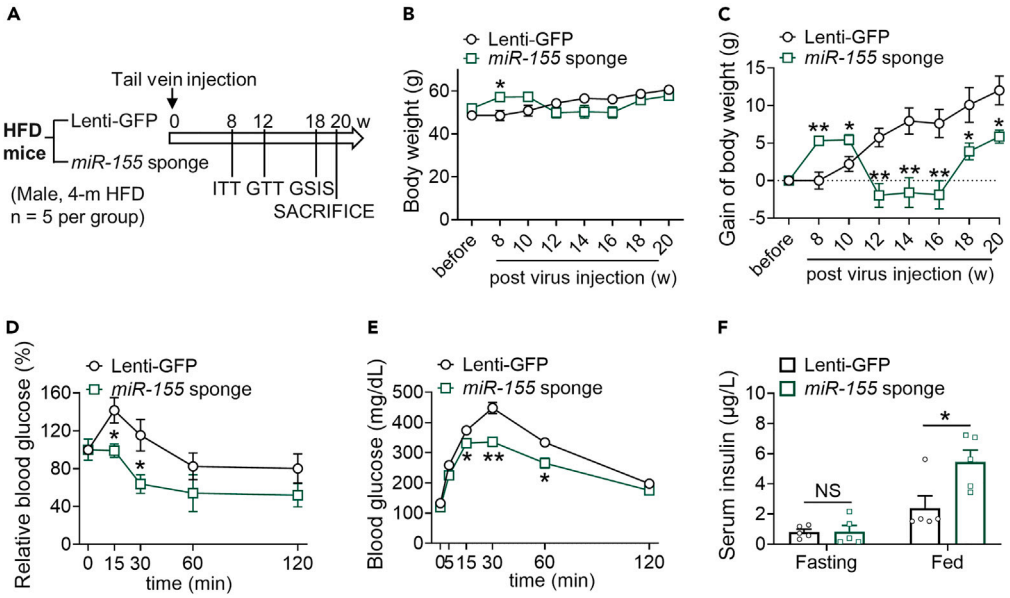

Figure 1. Inhibition of miR-155 ameliorates HFD-induced T2D pathogenesis in mice

(A) C57BL/6J male mice fed with 4-month HFD were injected with GFP or miR-155 sponge lentiviruses through tail vein. Experimental scheme to ascertain miR-155 sponge effects in HFD-induced T2D mouse model.

(B–E) Body weights (B), gain of body weights (C), ITTs (D), and GTTs (E) were performed in GFP and miR-155 sponge mice.

(F) Serum insulin levels were detected in GFP and miR-155 sponge mice under fasting or fed condition. Data were presented by Mean ± SEM. n = 5 per group. NS = not significant, *p < 0.05, **p < 0.01.

See also Figure S1.

RESULTS

Inhibition of miR-155 ameliorates HFD-induced T2D pathogenesis in mice

Previous studies have revealed miR-155 participates in T2D pathogenesis. Here, we examined whether inhibiting miR-155 could alleviate T2D symptoms in HFD-feeding mice by injecting miR-155 sponge lentiviruses after 4 months of HFD feeding (Figure 1A). The mice administered the miR-155 sponge showed a tendency to gain weight within 10 weeks after the injection, whereas the mice showed a dramatic reduction in weight gain after 12 weeks compared with the GFP controls (Figures 1B and 1C). Moreover, inhibition of miR-155 significantly improved HFD-induced insulin resistance and glucose intolerance (Figures 1D and 1E). Notably, although the serum insulin levels showed no obvious differences in the fasting condition, the levels were significantly increased after feeding (Figure 1F), indicating inhibition of miR-155 improved β cell function. We also determined that the administration of the miR-155 sponge significantly enhanced *in vivo* glucose-stimulated insulin secretion (GSIS) in HFD-feeding mice (Figure S1A). Overall, these results suggest that miR-155 inhibition ameliorates HFD-induced T2D pathogenesis in mice.

Inhibition of miR-155 increases islet mass and peripheral insulin signaling transduction

Islets mass is critical for the development of T2D under metabolic stress. Here, we examined islets mass to determine the mitigative effect of miR-155 inhibition on T2D symptoms in HFD-feeding mice by pancreatic hematoxylin and eosin (H&E) staining. Indeed, the islets were larger in size in the pancreases of HFD-feeding mice administered the miR-155 sponge than in the GFP controls (Figure 2A), and the ratio of islet area to pancreas area was also higher (Figure 2B). Large islets (>15 μm^2) were also more abundant in the pancreases of HFD-feeding mice treated with the miR-155 sponge (Figure 2C). Besides, β-catenin measurements showed that the sizes of β cell were larger in HFD mice with miR-155 sponge, which may contribute to the enlarged islet mass (Figures S1B and S1C). The greater islets mass could secret more insulin in turn to meet the demand for insulin in the peripheral tissues of HFD-feeding mice. Moreover, we observed that insulin signaling pathway was significantly activated in the peripheral tissues of HFD-feeding mice administered the miR-155 sponge, as evidenced by the elevation of P-AKT (Phosphorylated AKT) expression in the epididymal white adipose tissue (eWAT) and livers (Figure 2D) while P-INSR (Phosphorylated INSR) and P-GSK3β (Phosphorylated GSK3β) expression were also upregulated in the latter (Figure S1D). Interestingly, lentivirus-based miR-155 sponge decreases the level of miR-155 in the pancreas but not in the liver, eWAT, or muscle (Figure 2E), consistent with observation of GFP fluorescence in isolated islets (Figure S1E). Thus, these findings revealed that pancreatic miR-155 inhibition promoted islet mass enlargement and improved peripheral insulin sensitivity to ameliorate the symptoms of HFD-induced T2D.

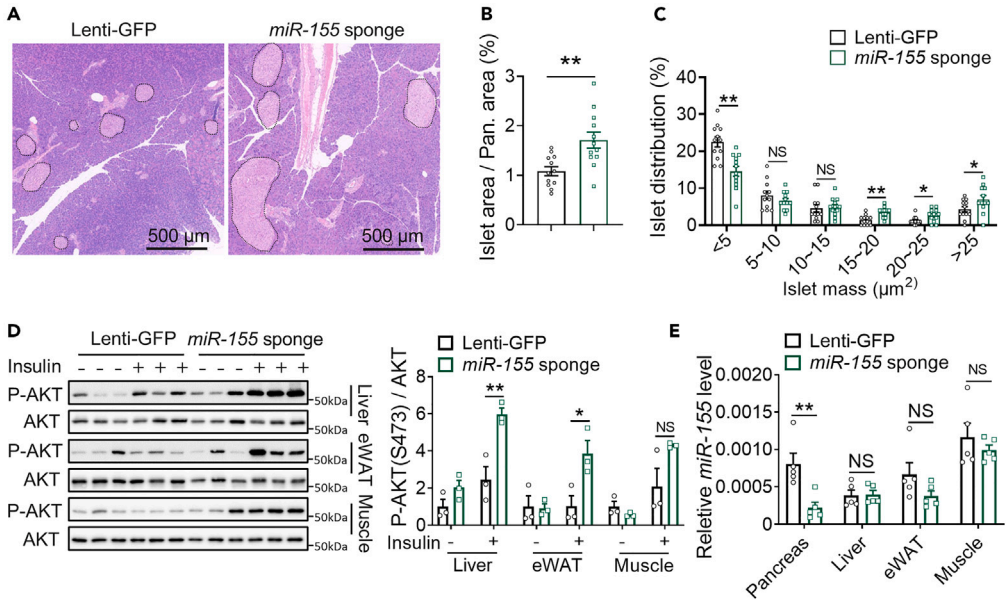

Figure 2. Inhibition of miR-155 increases islet mass and peripheral insulin signaling transduction

(A) Histopathological analysis of pancreas tissues. Mice injected with Lenti-GFP and miR-155 sponge lentiviruses for 4 months. Islet areas were assessed by H&E staining.

(B) The ratio of islet area to pancreatic area was calculated between the GFP and miR-155 sponge mice.

(C) The distribution of islets mass in GFP and miR-155 sponge mice.

(D) Representative western blot images (left) and quantitative analysis (right) of P-AKT and AKT in lysates of liver, eWAT, and muscles from GFP or miR-155 sponge mice with or without insulin stimulation.

(E) Relative miR-155 expression in pancreas, liver, eWAT, and muscle determined by qPCR. Data were presented by Mean ± SEM. n = 3–12 per group. NS = not significant, *p < 0.05, **p < 0.01.

See also Figure S1.

Increased miR-155 level in type-2 diabetic islets is derived from islet-resident macrophages

To clarify the role and source of elevated miR-155 in islets of T2D, we firstly performed single-cell RNA sequencing (scRNA-seq) of islets isolated from wild-type mice to determine the location of miR-155. Based on specific marker gene expression, we identified distinct clusters representing β cells, α/δ/PP cells, endothelial cells, and macrophages, as shown by the heatmap (Figure 3A). MiR155hg, a long noncoding RNA, is the host gene of miR-155 and co-regulates with it. MiR155hg was co-expressed with inflammatory factor interleukin (IL)-1β and IL-6, as well as with the macrophage biomarker adgre1 (Figures 3B and S2D), suggesting that miR-155 was mainly expressed in islet macrophages. Previous studies have revealed that the infiltration of macrophages into islets increases with the progression of T2D. Consistently, we detected a significant upregulation of miR-155 in the islets of 12- or 18-week-old HFD-feeding mice (Figure 3C) and 8- or 12-week-old db/db mice with obesity and hyperglycemia (Figures 3D and S2A–S2C). Similarly, the expression of miR-155 was markedly elevated in human islets treated with palmitic acid (Figure 3E). We also tested whether the elevated miR-155 in diabetic islets was derived from resident macrophages by administering clodronate liposomes (C-lipos) to clear macrophages from the islets of both db/db mice and humans, as evidenced by the reduction of macrophages maker genes level (Figures S2E and S2F). Meanwhile, C-lipos did not affect glucose-stimulated insulin secretion in human islets (Figure S2G). Surprisingly, miR-155 expression was significantly decreased in the islets of db/db mice and humans with C-lipo treatment (Figures 3F and 3G). Collectively, the data supported the notion that the increased levels of miR-155 in diabetic islets were derived from resident macrophages.

MiR-155 mimics inflammation-induced β cell dysfunction

Next, we investigated whether macrophage-derived miR-155 impaired insulin secretion by overexpressing miR-155 in β cells and islets. Initially, we observed that miR-155 overexpression decreased GSIS and potassium-stimulated insulin secretion (KSIS) in Min6 cells (Figure 4A), while also inhibiting cell viability without inducing apoptosis, as determined by Cell Counting Kit-8 (CCK8) and Hoechst staining (Figures S4A and S4B). Moreover, miR-155 also reduced dynamic insulin secretion in islets during glucose perfusion (Figure 4B) and impaired GSIS in human islets (Figure 4C). Intriguingly, although KSIS was little effected in INS-1 cells (Figure S4C), insulin content was significantly decreased after miR-155 transfection (Figure 4D), along with downregulated Ins1 and Ins2 gene levels as well as decreased cell viability (Figures 4E and S4D). Similarly, miR-155 also decreased insulin content in human islets (Figure 4F). One interesting finding was that blocking miR-155

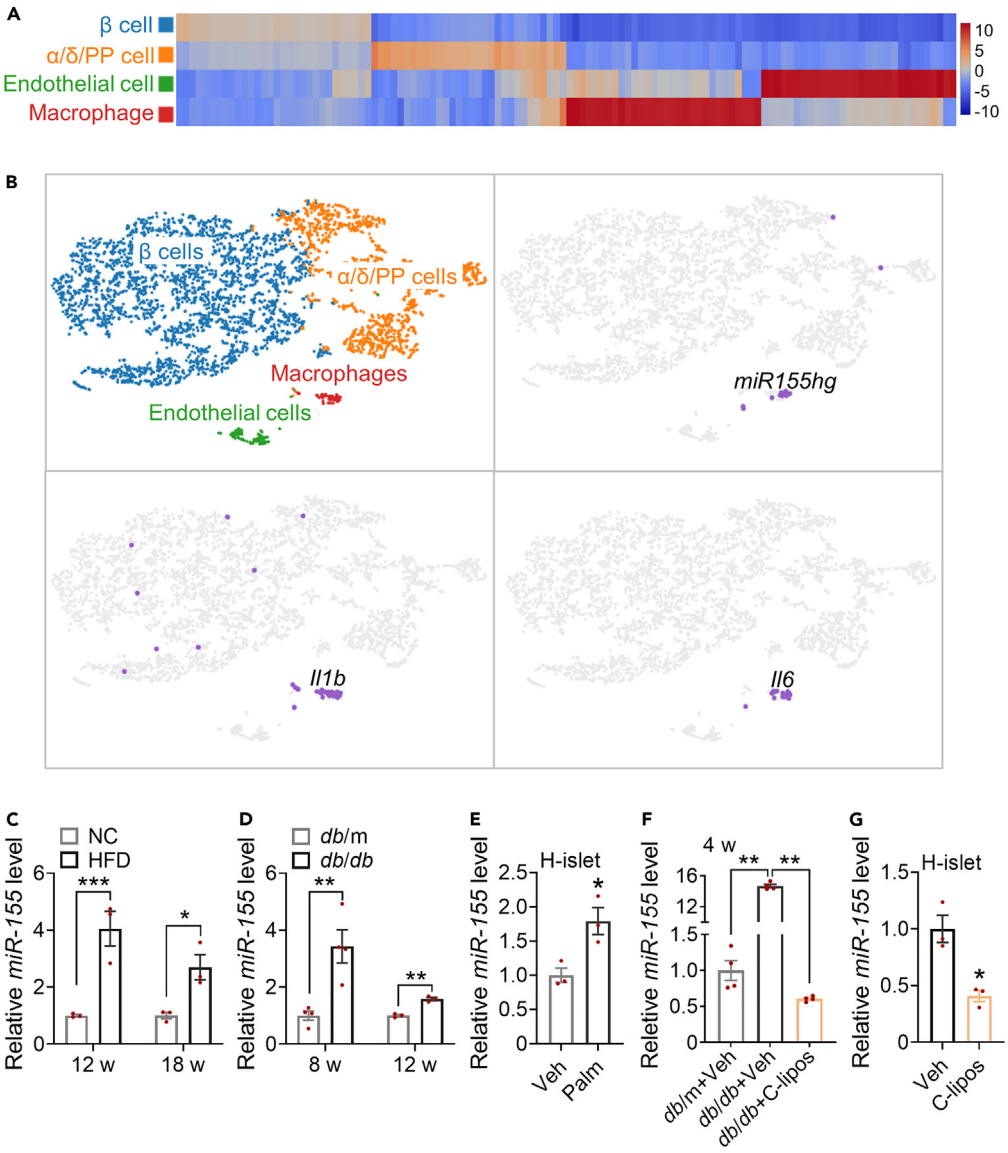

Figure 3. Increased miR-155 in type-2 diabetic islets is derived from islet-resident macrophages

(A) Whole-islet scRNA-seq was performed in WT mice, and β cell, α/δ/PP cell, endothelial cell, and macrophage clusters were classified according to the heatmap of characteristic gene expression in different cells.

(B) The distribution of four clusters corresponding to the whole-islet sequencing map, and the distribution of miR155hg, IL-1β, and IL-6 in islets was also labeled.

(C and D) Relative miR-155 levels in islets of 12- or 18-week HFD mice (C) and 8- or 12-week db/db mice (D), compared with that in control mice, respectively.

(E) Relative miR-155 levels in human islets with and without Palm treatment.

(F) Relative miR-155 levels in islets of 4-week db/m mice, db/db mice with or without C-lipos treatment.

(G) Relative miR-155 levels in human islets with or without C-lipos treatment. Data were presented by Mean ± SEM. n = 3–4 per group. *p < 0.05, **p < 0.01, ***p < 0.001.

See also Figure S2.

in IL-1β-treated islets improved insulin secretion and content (Figures 4G and 4H), indicating miR-155 can mimic inflammation-induced β cell dysfunction. Besides, although insulin content had little changes (Figure S3A), miR-155 inhibition clearly increased GSIS in db/db islets (Figure 4I).

Further, we observed mainly pro-inflammatory M1 macrophages increased in islets of 12-week db/db mice compared with 4-week, as evidenced by the elevation of adgre1 expression (M1 marker) rather than mrc1 (M2 marker) (Figure S3B). Indeed, both M1 macrophage and its exosomes (M1-exo) had more than 20 times expression levels of miR-155 compared to M0, M2 macrophages and their relative exosomes (M2-exo and M0-exo) (Figure S3C). Moreover, M1-exo could enter β cells to impair GSIS function (Figures S3D–S3F). More importantly, miR-155

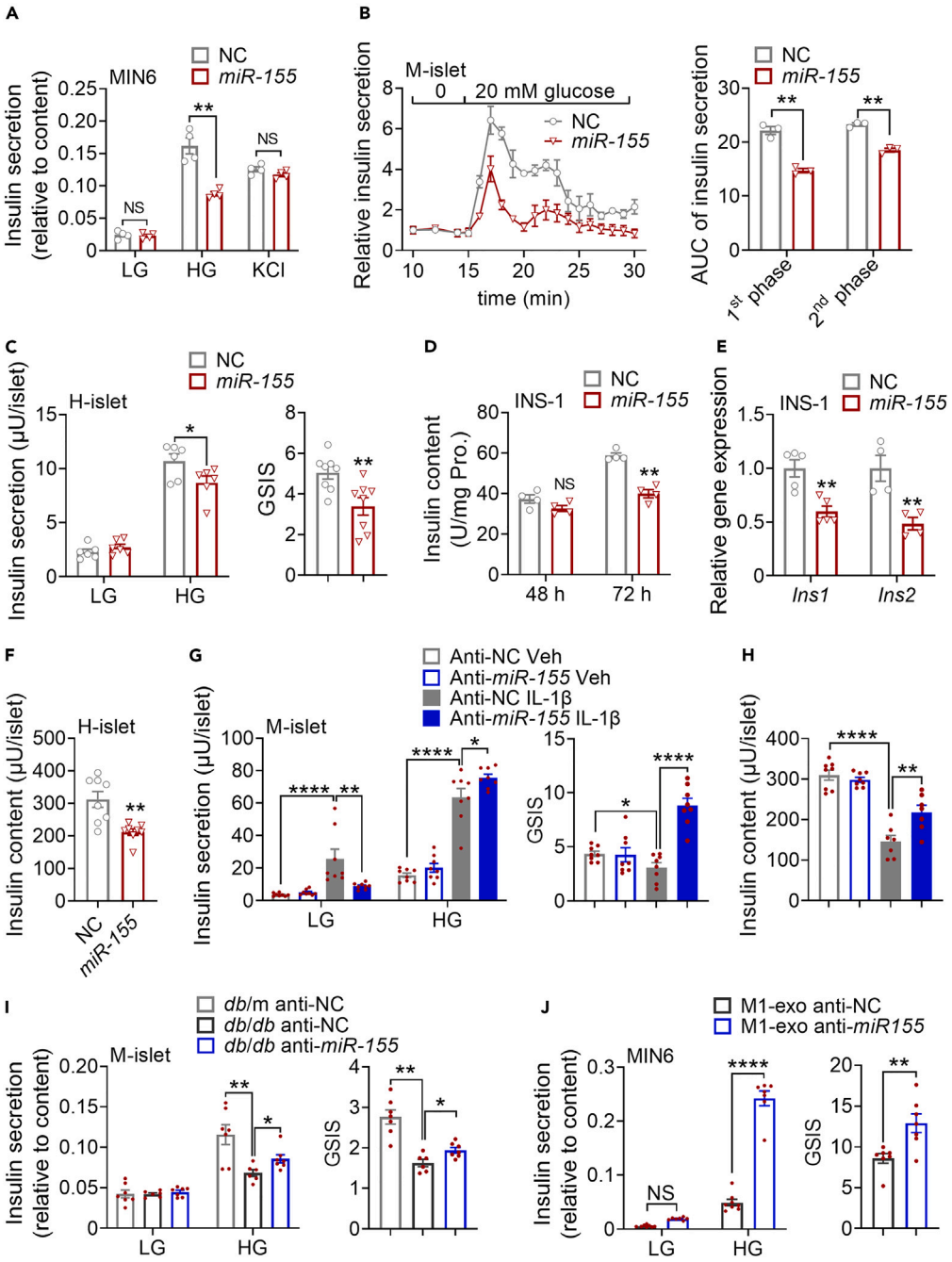

Figure 4. miR-155 mimics inflammation-induced β cell dysfunction

(A) The ratio of insulin secretion to content in Min6 cells transfected with miR-155 under low-glucose, high-glucose, and high-potassium condition.

(B) Islets perfusion was performed after miR-155 transfection for 48 h (left). The AUC (Area under the curve) of the first phase (from 10 to 20 min) and the second phase (20–30 min) of insulin secretion was analyzed by GraphPad prism 8.

(C) Insulin secretion detection (left) and glucose-stimulated index (GSI) calculation (right) in human islets transfected with miR-155 under low- and high-glucose condition, respectively.

(D) Insulin content corrected by protein concentration was examined in INS-1 after miR-155 transfection for 48 h and 72 h.

(E) Relative Ins1 and Ins2 mRNA expression in INS-1 cells after miR-155 transfection for 48 h.

(F) Insulin content of human islets transfected miR-155 or NC.

(G) Insulin secretion per islet (left) and GSIS ratio (right) detection in mice islets treated with IL-1β with or without miR-155 blocking.

(H) Insulin content was examined in mice islets treated with IL-1β with or without miR-155 blocking.

(I) Insulin secretion (left) and GSIS ratio (right) detection in db/db islets with or without miR-155 blocking.

Figure 4. *Continued*

(J) Insulin secretion (left) and GSIS ratio (right) detection in Min6 cells treated with M1-derived exosomes with or without miR-155 blocking. Data were presented by Mean ± SEM. n = 3–8 per group. NS = not significant, *p < 0.05, **p < 0.01, ***p < 0.001, ****p < 0.0001.
See also Figures S3 and S4.

blocking in M1-exos dramatically decreased miR-155 level and rescued the expression of genes associated with insulin transcription and increased GSIS in Min6 cells (Figures S3G, S3H, and 4J). Taken together, these results demonstrated that miR-155 derived from pro-inflammatory M1 macrophages induced β cell dysfunction which could be rescued by miR-155 inhibition of M1-exos.

MiR-155-PDX1 axis mediates impairments from islet inflammation

Mechanistically, our use of the TargetScan prediction website and luciferase reporter assays revealed that miR-155 directly targeted and inhibited the expression of a key transcription factor, PDX1, by binding to its 3′ UTR (Figures 5A and 5B). This finding was consistent with the downregulation of PDX1 at the protein level in Min6 cells after miR-155 transfection (Figure 5C). In contrast, inhibition of miR-155 markedly increased the expression of PDX1 in islets of db/db mice (Figure 5D). Moreover, miR-155 sponge treatment also upregulated PDX1 expression relative to Ins1 in the pancreases of HFD-feeding mice (Figures 5E and 5F), whereas the genes of macrophage maker were decreased markedly (Figure S5A). After clearing macrophages by C-lipo treatment (Figures S5B–S5D), we observed PDX1 expression was rescued in islets of HFD-feeding mice and in 4-week-old and 12-week-old db/db mice (Figures 5G and 5H), indicating that an miR-155-PDX1 axis mediated the impairment of islet inflammation. In addition, overexpression of PDX1 rescued the impaired GSIS caused by miR-155 in Min6 cells (Figures 5I and 5J). Taken together, these findings indicated that miR-155 inhibited β cell dysfunction by targeting PDX1.

Inhibition of miR-155 treats type-2 diabetic db/db mice

We also tested whether miR-155 inhibition by antagomiR-155 injection via abdominal aorta could treat type-2 diabetic db/db mice. We observed that db/db mice administered antagomiR-155 showed lowered random blood glucose levels (Figure 6A), improved glucose tolerance and insulin sensitivity, and increased insulin secretion compared with that in controls (Figures 6C–6F), although no significant difference was noted in body weight (Figure 6B). In addition, we also determined the effect of miR-155 on the features of T1D. The expression of miR-155 was significantly increased in the islets and infiltrated lymphocytes of NOD mice (Figures S6A and S6B) and was induced by inflammatory factors (IL-1β, either alone or combined with tumor necrosis factor alpha [TNF-α] and interferon gamma [IFNγ]) (Figure S6C). Furthermore, administration of the miR-155 sponge dramatically reduced diabetic morbidity and mortality in NOD mice (Figures S6D and S6E). In summary, our findings identified miR-155 as a promising therapeutic target for both T2D and T1D.

DISCUSSION

Extensive studies have reported the dysregulation of miR-155 expression in serum and peripheral blood mononuclear cells in patients with T2D diabetes[29,30]; however, its level and role in type-2 diabetic islets have not been intensively explored. A previous study reported that hyperlipidemia-associated endotoxemia-induced miR-155-5p targeted mafb in β cells to promote IL-6 expression, which further increased the GLP (glucagon-like peptide) level and thereby increased insulin secretion.[31] In contrast, Regazzi et al. have revealed that lymphocyte-derived exosomal miR-155 promoted pancreatic β cell death and contributed to T1D development,[28] indicating that the effect of miR-155 on β cell function was also obscure. In this study, we demonstrated that the expression of miR-155 was significantly elevated in islets of HFD-feeding and type-2 diabetic db/db mice (Figure 3), and overexpression of miR-155 decreased insulin secretion and content both in β cell lines and pancreatic islets (Figure 4), indicating the increase of miR-155 in islets under metabolic stress promotes T2D progression.

Obesity is an independent risk factor for T2D. In HFD-feeding mice, body weight gain triggers adaptive islet expansion to compensate for peripheral insulin resistance;[32] once the expansion is insufficient, it will develop into typical T2D. We considered that intervention at the compensatory stage could delay or prevent the development of T2D. Here, we observed that blocking miR-155 increased single β cell size and islets mass in HFD-feeding mice, which in turn compensated for the insulin resistance by releasing more insulin (Figures 2 and S1). A previous study reported by Lin has shown that, under the normal chow diet condition, no significant difference was observed on β cell proliferation, mass, and insulin genes expression between global miR-155 knockout (KO) mice and control mice.[33] These phenotypes suggest that the effect of miR-155 on islets is mainly in the pathological state rather than in the physiological, and its upregulation in islets of obese individual may accelerate the course of diabetes, while inhibition of miR-155 can treat T2D. Here, we used miRNA sponge to inhibit miR-155 expression in HFD mice. We observed that miR-155 levels were reduced by half in the pancreases of HFD mice after miR-155 sponge lentiviruses injection (Figure 2), which indicated that the method we used was effective. In addition, there are also other ways to suppress miRNA expression *in vivo* or *in vitro*, such as the antagomir-155 we used in db/db mice as well as bulged sponge reported by Gao et al.[34] It is hoped to introduce multiple strategies for miRNA intervention in future studies.

Several studies have demonstrated the pro-inflammatory effects of miR-155 on multiple disease.[35,36] Interestingly, almost all the pro-inflammatory effects of miR-155 are associated with macrophages.[20,35–39] Wang et al. have reported that miR-155-containing macrophage exosomes promoted inflammation in cardiac fibroblasts by suppressing anti-inflammatory gene SOCS1,[36] and inflammatory macrophages-derived miR-155 in obese adipose tissue promoted insulin resistance by targeting PPARγ in the livers and muscle,[20] indicating that miR-155 facilitated inflammation by multiple mechanisms. Insulitis dominated by macrophage was also an inflammatory manifestation in T2D. Macrophages induce β cell dysfunction through a variety of pathways, including secreting pro-inflammatory factors and transferring inflammatory

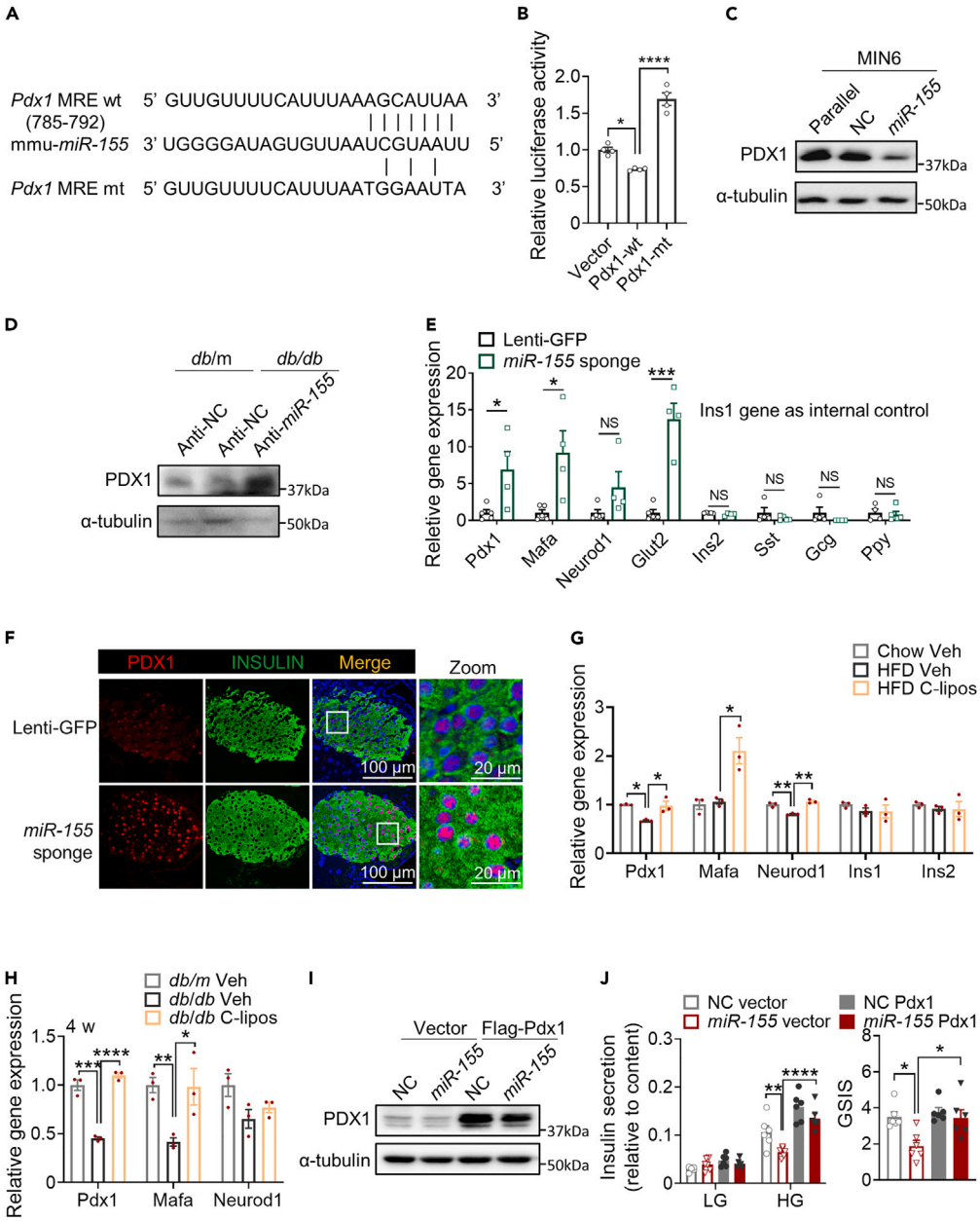

Figure 5. miR-155-PDX1 mediates impairments from islet inflammation

(A and B) Sequence matching between PDX1and miR-486 (A) and dual luciferase reporter test (B).

(C and D) Representative western blot images of PDX1 expression in Min6 cells transfected with miR-155 (C) and islets of db/db mice (D) treated with miR-155 inhibition.

(E) Relative genes expression corrected by Ins1 was quantified in pancreas of HFD mice with lenti-GFP and miR-155 sponge.

(F) PDX1 (red) and insulin (green) staining in in pancreatic islets of mice with lenti-GFP and miR-155 sponge.

(G and H) Relative genes expression in islets of HFD (G) and db/db mice (H) with C-lipos treatment.

(I) Representative western blot images of PDX1 expression in Min6 cells transfected with miR-155 with or without PDX1 overexpression.

(J) Insulin secretion (left) and GSIS ratio (right) detection in Min6 cells transfected with miR-155 with or without PDX1 overexpression under low- or high-glucose condition. Data were presented by Mean ± SEM. n = 3–6 per group. NS = not significant, *p < 0.05, **p < 0.01, ***p < 0.001, ****p < 0.0001.

See also Figure S5.

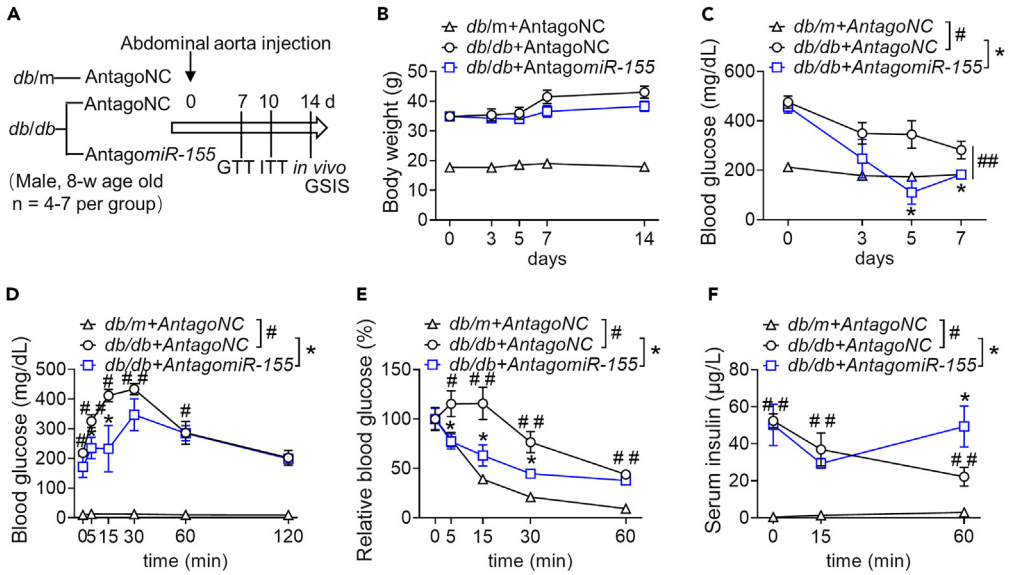

Figure 6. Inhibition of miR-155 treats type-2 diabetic db/db mice

(A) Db/db male mice were injected AntagoNC or AntagomiR-155 via abdominal aorta at 8 weeks and further monitored metabolic index following the experimental scheme.

(B–F) The measurement of body weights (B), blood glucose (C), GTTs (D), ITTs (E), and serum insulin (F) in db/m and db/db mice with AntagoNC or AntagomiR-155 injection. Data were presented by Mean ± SEM. n = 4–7 per group. *p < 0.05. #p < 0.01, ##p < 0.001.

See also Figure S6.

mitochondria[40] and miRNAs to β cells by extracellular vesicles. In this study, we investigated miR-155 derived from islet-resident macrophages impaired β cell function via targeting PDX1, which is a characteristic gene of β cells involving in insulin synthesis and secretion. We also observed increased PDX1 expression and improved β cell function in HFD mice injected with miR-155 sponge lentivirus, indicating that the role of blocking miR-155 in the treatment of T2D was depended on PDX1 expression in β cells, while it might be independent of inflammatory effects. Besides, a study has reported that blockade of lymphocyte-derived miRNAs (including miR-142, miR-150, and miR-155) decreases diabetes incidence in NOD mice.[28] Intriguingly, we discovered that inhibition of miR-155 alone also exerted therapeutic effect on NOD mice (Figures S6D and S6E). However, the mechanism of miR-155 in treating T1D was unclear and needed further study.

The origin of islet miR-155 depends on islet microenvironment. Normally, islet-resident macrophages are the main source of miR-155 as evidenced by our scRNA-seq, at least in C57BL/6J mouse islets (Figure 3). During the development of T1D and T2D, distinct immune cell types,[16] such as lymphocytes and macrophages in type-1 diabetic islets as well as macrophages in type-2 diabetic islets, contribute to the increased levels of islet miR-155. Despite the different origins of miR-155 in the T1D and T2D disease statuses, engulfed miR-155 by β cells led to the insufficient insulin secretion and/or insulin resistance, which could be treated by our lentivirus-based miR-155 sponge strategy. Therefore, we employed three kind of diabetic mouse models (HFD, db/db, and NOD) to prove the anti-diabetic effects via blocking islet miR-155 regardless of the origins.

In summary, our study demonstrated that aberrantly increased miR-155 derived from M1 macrophages caused islet inflammation and impaired β cell function during T2D progression, whereas inhibition of MDE-miR-155 alleviated β cell dysfunction. *In vivo*, blocking miR-155 increased insulin secretion and improved glucose tolerance and insulin sensitivity in HFD-feeding and type-2 diabetic db/db mice. Overall, therapeutic strategies aimed at blocking miR-155 in macrophages represent a promising approach for the prevention and treatment of obesity-induced T2D.

Limitations of the study

Here, we discovered that PDX1 was the vital target gene of miR-155 which caused the defects in β cell GSIS function and insulin biosynthesis in the development of T2D; however, we also observed that β cell sizes were enlarged in islet of HFD-feeding mice with miR-155 sponge, indicating potential target genes might play an important role to understand how miR-155 regulated β cell size. In addition, previous studies have revealed that silencing miR-155 can inhibit M1 macrophage polarization that reduces inflammation.[41,42] Our work focused on M1 macrophage-derived exosomal miR-155 entering β cells and contributing to β cell dysfunction, in which we neglected the effect of miR-155 sponge on M1 macrophage polarization that might also delay the progression of T2D.

STAR★METHODS

Detailed methods are provided in the online version of this paper and include the following:

- KEY RESOURCES TABLE
- RESOURCE AVAILABILITY
  - Lead contact
  - Materials availability
  - Data and code availability
- EXPERIMENTAL MODEL AND STUDY PARTICIPANT DETAILS
  - Animals
  - Primary islet isolation and cell culture
- METHOD DETAILS
  - Tail vein injection and abdomens aorta injection
  - Islet-resident macrophage clearance
  - Metabolic characters and ELISA
  - Insulin sensitivity assays
  - Immunofluorescence staining
  - Bone marrow-derived macrophage isolation
  - BMDM-derived exosomes isolation
  - Exosomes transfection
  - Fluorescence labeling of exosomes
  - GSIS, KSIS and islet perfusion assay
  - Western blot analysis
  - RNA extraction and qPCR
  - Plasmid construction and luciferase assay
  - Single-cell RNA sequencing (scRNA-seq)
- QUANTIFICATION AND STATISTICAL ANALYSIS

SUPPLEMENTAL INFORMATION

Supplemental information can be found online at https://doi.org/10.1016/j.isci.2024.109540.

ACKNOWLEDGMENTS

This study was supported by research grants from the National Natural Science Foundation of China, China (Grant numbers: 82330027, 82070843,and 82270844). X.H. and Y. Zhu are fellows at the Collaborative Innovation Center for Cardiovascular Disease Translational Medicine, China. We thank Prof. Shusen Wang (Organ Transplant Center, NHC Key Laboratory for Critical Care Medicine, Tianjin First Central Hospital, Nankai University, Tianjin, China) for providing human islet sample. Thanks to BioRender software (http://biorender.com), the graphical abstract was created with BioRender.com with permission.

AUTHOR CONTRIBUTIONS

Conceptualization, X.H. and Y. Zhu; methodology, Y. Zhang, R.C., and T.L.; investigation, T.L. and K.L.; formal analysis, Y. Zhang, K.L., and Y.L.; writing – original draft, Y. Zhang and R.C.; writing – review and editing, Y. Zhu; funding acquisition, X.H. and Y. Zhu; resources, X.C.; supervision, X.H. and Y. Zhu.

DECLARATION OF INTERESTS

The authors declare no competing interests.

Received: October 6, 2023
Revised: February 18, 2024
Accepted: March 18, 2024
Published: March 20, 2024

REFERENCES

1. Hudish, L.I., Reusch, J.E., and Sussel, L. (2019). β Cell dysfunction during progression of metabolic syndrome to type 2 diabetes. J. Clin. Invest. *129*, 4001–4008. https://doi.org/10.1172/jci129188.
2. Kahn, S.E., Hull, R.L., and Utzschneider, K.M. (2006). Mechanisms linking obesity to insulin resistance and type 2 diabetes. Nature *444*, 840–846. https://doi.org/10.1038/nature05482.
3. Avrahami, D., Wang, Y.J., Schug, J., Feleke, E., Gao, L., Liu, C., HPAP Consortium, Naji, A., Glaser, B., and Kaestner, K.H. (2020). Single-cell transcriptomics of human islet ontogeny defines the molecular basis of β-cell dedifferentiation in T2D. Mol. Metab. *42*, 101057. https://doi.org/10.1016/j.molmet.2020.101057.
4. Saisho, Y. (2014). Importance of Beta Cell Function for the Treatment of Type 2 Diabetes. J. Clin. Med. *3*, 923–943. https://doi.org/10.3390/jcm3030923.
5. Ding, L., Zhang, Y., Wang, Y., Wang, Y., Tong, Z., Li, P., Chen, C., Wang, B., Yue, X., Li, C.,

et al. (2023). Zhx2 maintains islet β-cell mass and function by transcriptionally regulating Pax6. iScience *26*, 106871. https://doi.org/10.1016/j.isci.2023.106871.

6. Donath, M.Y., Böni-Schnetzler, M., Ellingsgaard, H., Halban, P.A., and Ehses, J.A. (2010). Cytokine production by islets in health and diabetes: cellular origin, regulation and function. Trends Endocrinol. Metab. *21*, 261–267. https://doi.org/10.1016/j.tem.2009.12.010.
7. Stumvoll, M., Goldstein, B.J., and van Haeften, T.W. (2005). Type 2 diabetes: principles of pathogenesis and therapy. Lancet (London, England) *365*, 1333–1346. https://doi.org/10.1016/s0140-6736(05)61032-x.
8. Talchai, C., Xuan, S., Lin, H.V., Sussel, L., and Accili, D. (2012). Pancreatic β cell dedifferentiation as a mechanism of diabetic β cell failure. Cell *150*, 1223–1234. https://doi.org/10.1016/j.cell.2012.07.029.
9. Gunton, J.E. (2020). Hypoxia-inducible factors and diabetes. J. Clin. Invest. *130*, 5063–5073. https://doi.org/10.1172/jci137556.
10. Richardson, S.J., Willcox, A., Bone, A.J., Foulis, A.K., and Morgan, N.G. (2009). Islet-associated macrophages in type 2 diabetes. Diabetologia *52*, 1686–1688. https://doi.org/10.1007/s00125-009-1410-z.
11. Ying, W., Lee, Y.S., Dong, Y., Seidman, J.S., Yang, M., Isaac, R., Seo, J.B., Yang, B.H., Wollam, J., Riopel, M., et al. (2019). Expansion of Islet-Resident Macrophages Leads to Inflammation Affecting β Cell Proliferation and Function in Obesity. Cell Metabol. *29*, 457–474.e5. https://doi.org/10.1016/j.cmet.2018.12.003.
12. Cucak, H., Grunnet, L.G., and Rosendahl, A. (2014). Accumulation of M1-like macrophages in type 2 diabetic islets is followed by a systemic shift in macrophage polarization. J. Leukoc. Biol. *95*, 149–160. https://doi.org/10.1189/jlb.0213075.
13. Westwell-Roper, C.Y., Ehses, J.A., and Verchere, C.B. (2014). Resident macrophages mediate islet amyloid polypeptide-induced islet IL-1β production and β-cell dysfunction. Diabetes *63*, 1698–1711. https://doi.org/10.2337/db13-0863.
14. Calderon, B., Carrero, J.A., Ferris, S.T., Sojka, D.K., Moore, L., Epelman, S., Murphy, K.M., Yokoyama, W.M., Randolph, G.J., and Unanue, E.R. (2015). The pancreas anatomy conditions the origin and properties of resident macrophages. J. Exp. Med. *212*, 1497–1512. https://doi.org/10.1084/jem.20150496.
15. He, W., Yuan, T., and Maedler, K. (2019). Macrophage-associated pro-inflammatory state in human islets from obese individuals. Nutr. Diabetes *9*, 36. https://doi.org/10.1038/s41387-019-0103-z.
16. Ying, W., Fu, W., Lee, Y.S., and Olefsky, J.M. (2020). The role of macrophages in obesity-associated islet inflammation and β-cell abnormalities. Nat. Rev. Endocrinol. *16*, 81–90. https://doi.org/10.1038/s41574-019-0286-3.
17. Luc, K., Schramm-Luc, A., Guzik, T.J., and Mikolajczyk, T.P. (2019). Oxidative stress and inflammatory markers in prediabetes and diabetes. J. Physiol. Pharmacol. *70*. https://doi.org/10.26402/jpp.2019.6.01.
18. Charlton, B., Bacelj, A., and Mandel, T.E. (1988). Administration of silica particles or anti-Lyt2 antibody prevents beta-cell destruction in NOD mice given cyclophosphamide. Diabetes *37*, 930–935. https://doi.org/10.2337/diab.37.7.930.
19. Ortis, F., Pirot, P., Naamane, N., Kreins, A.Y., Rasschaert, J., Moore, F., Théâtre, E., Verhaeghe, C., Magnusson, N.E., Chariot, A., et al. (2008). Induction of nuclear factor-kappaB and its downstream genes by TNF-alpha and IL-1beta has a pro-apoptotic role in pancreatic beta cells. Diabetologia *51*, 1213–1225. https://doi.org/10.1007/s00125-008-0999-7.
20. Ying, W., Riopel, M., Bandyopadhyay, G., Dong, Y., Birmingham, A., Seo, J.B., Ofrecio, J.M., Wollam, J., Hernandez-Carretero, A., Fu, W., et al. (2017). Adipose Tissue Macrophage-Derived Exosomal miRNAs Can Modulate In Vivo and In Vitro Insulin Sensitivity. Cell *171*, 372–384.e12. https://doi.org/10.1016/j.cell.2017.08.035.
21. Qian, B., Yang, Y., Tang, N., Wang, J., Sun, P., Yang, N., Chen, F., Wu, T., Sun, T., Li, Y., et al. (2021). M1 macrophage-derived exosomes impair beta cell insulin secretion via miR-212-5p by targeting SIRT2 and inhibiting Akt/GSK-3β/β-catenin pathway in mice. Diabetologia *64*, 2037–2051. https://doi.org/10.1007/s00125-021-05489-1.
22. (2021). Tissue Macrophages Modulate Obesity-Associated β Cell Adaptations through Secreted miRNA-Containing Extracellular Vesicles. Cells *10*, 2451. https://doi.org/10.3390/cells10092451.
23. Zhang, Y., Mei, H., Chang, X., Chen, F., Zhu, Y., and Han, X. (2016). Adipocyte-derived microvesicles from obese mice induce M1 macrophage phenotype through secreted miR-155. J. Mol. Cell Biol. *8*, 505–517. https://doi.org/10.1093/jmcb/mjw040.
24. Kim, N.H., Ahn, J., Choi, Y.M., Son, H.J., Choi, W.H., Cho, H.J., Yu, J.H., Seo, J.A., Jang, Y.J., Jung, C.H., and Ha, T.Y. (2020). Differential circulating and visceral fat microRNA expression of non-obese and obese subjects. Clin. Nutr. *39*, 910–916. https://doi.org/10.1016/j.clnu.2019.03.033.
25. Gao, J., Zhao, G., Li, W., Zhang, J., Che, Y., Song, M., Gao, S., Zeng, B., and Wang, Y. (2018). MiR-155 targets PTCH1 to mediate endothelial progenitor cell dysfunction caused by high glucose. Exp. Cell Res. *366*, 55–62. https://doi.org/10.1016/j.yexcr.2018.03.012.
26. Wang, L., and Cao, Q.M. (2022). Long non-coding RNA XIST alleviates sepsis-induced acute kidney injury through inhibiting inflammation and cell apoptosis via regulating miR-155-5p/WWC1 axis. Kaohsiung J. Med. Sci. *38*, 6–17. https://doi.org/10.1002/kjm2.12442.
27. Qu, B., He, J., Zeng, Z., Yang, H., Liu, Z., Cao, Z., Yu, H., Zhao, W., and Pan, X. (2020). MiR-155 inhibition alleviates suppression of osteoblastic differentiation by high glucose and free fatty acids in human bone marrow stromal cells by upregulating SIRT1. Pflugers Arch. *472*, 473–480. https://doi.org/10.1007/s00424-020-02372-7.
28. Guay, C., Kruit, J.K., Rome, S., Menoud, V., Mulder, N.L., Jurdzinski, A., Mancarella, F., Sebastiani, G., Donda, A., Gonzalez, B.J., et al. (2019). Lymphocyte-Derived Exosomal MicroRNAs Promote Pancreatic β Cell Death and May Contribute to Type 1 Diabetes Development. Cell Metabol. *29*, 348–361.e6. https://doi.org/10.1016/j.cmet.2018.09.011.
29. Jankauskas, S.S., Gambardella, J., Sardu, C., Lombardi, A., and Santulli, G. (2021). Functional Role of miR-155 in the Pathogenesis of Diabetes Mellitus and Its Complications. Noncoding. RNA *7*, 39. https://doi.org/10.3390/ncrna7030039.
30. Hu, J., Huang, S., Liu, X., Zhang, Y., Wei, S., and Hu, X. (2022). miR-155: An Important Role in Inflammation Response. J. Immunol. Res. *2022*, 7437281. https://doi.org/10.1155/2022/7437281.
31. Zhu, M., Wei, Y., Geißler, C., Abschlag, K., Corbalán Campos, J., Hristov, M., Möllmann, J., Lehrke, M., Karshovska, E., and Schober, A. (2017). Hyperlipidemia-Induced MicroRNA-155-5p Improves β-Cell Function by Targeting Mafb. Diabetes *66*, 3072–3084. https://doi.org/10.2337/db17-0313.
32. Ji, Y., Sun, S., Shrestha, N., Darragh, L.B., Shirakawa, J., Xing, Y., He, Y., Carboneau, B.A., Kim, H., An, D., et al. (2019). Toll-like receptors TLR2 and TLR4 block the replication of pancreatic β cells in diet-induced obesity. Nat. Immunol. *20*, 677–686. https://doi.org/10.1038/s41590-019-0396-z.
33. Lin, X., Qin, Y., Jia, J., Lin, T., Lin, X., Chen, L., Zeng, H., Han, Y., Wu, L., Huang, S., et al. (2016). MiR-155 Enhances Insulin Sensitivity by Coordinated Regulation of Multiple Genes in Mice. PLoS Genet. *12*, e1006308. https://doi.org/10.1371/journal.pgen.1006308.
34. Shao, Y., Wu, W., Fan, F., Liu, H., Ming, Y., Liao, W., Bai, C., and Gao, Y. (2023). Extracellular Vesicle Content Changes Induced by Melatonin Promote Functional Recovery of Pancreatic Beta Cells in Acute Pancreatitis. J. Inflamm. Res. *16*, 6397–6413. https://doi.org/10.2147/jir.S430916.
35. Bala, S., Csak, T., Saha, B., Zatsiorsky, J., Kodys, K., Catalano, D., Satishchandran, A., and Szabo, G. (2016). The pro-inflammatory effects of miR-155 promote liver fibrosis and alcohol-induced steatohepatitis. J. Hepatol. *64*, 1378–1387. https://doi.org/10.1016/j.jhep.2016.01.035.
36. Wang, C., Zhang, C., Liu, L., A, X., Chen, B., Li, Y., and Du, J. (2017). Macrophage-Derived mir-155-Containing Exosomes Suppress Fibroblast Proliferation and Promote Fibroblast Inflammation during Cardiac Injury. Mol. Ther. *25*, 192–204. https://doi.org/10.1016/j.ymthe.2016.09.001.
37. Zhang, Z., Chen, H., Zhou, L., Li, C., Lu, G., and Wang, L. (2022). Macrophage-derived exosomal miRNA-155 promotes tubular injury in ischemia-induced acute kidney injury. Int. J. Mol. Med. *50*, 116. https://doi.org/10.3892/ijmm.2022.5172.
38. Wang, B., Wang, Z.M., Ji, J.L., Gan, W., Zhang, A., Shi, H.J., Wang, H., Lv, L., Li, Z., Tang, T., et al. (2020). Macrophage-Derived Exosomal Mir-155 Regulating Cardiomyocyte Pyroptosis and Hypertrophy in Uremic Cardiomyopathy. JACC. Basic Transl. Sci. *5*, 148–166. https://doi.org/10.1016/j.jacbts.2019.10.011.
39. Ge, X., Tang, P., Rong, Y., Jiang, D., Lu, X., Ji, C., Wang, J., Huang, C., Duan, A., Liu, Y., et al. (2021). Exosomal miR-155 from M1-polarized macrophages promotes EndoMT and impairs mitochondrial function via activating NF-κB signaling pathway in vascular endothelial cells after traumatic spinal cord injury. Redox Biol. *41*, 101932. https://doi.org/10.1016/j.redox.2021.101932.
40. Gao, Y., Mi, N., Wu, W., Zhao, Y., Fan, F., Liao, W., Ming, Y., Guan, W., and Bai, C. (2024). Transfer of inflammatory mitochondria via extracellular vesicles from M1 macrophages induces ferroptosis of pancreatic beta cells in acute pancreatitis. J. Extracell. Vesicles *13*, e12410. https://doi.org/10.1002/jev2.12410.
41. Wang, H., Zhang, H., Fan, K., Zhang, D., Hu, A., Zeng, X., Liu, Y.L., Tan, G., and Wang, H.

(2021). Frugoside delays osteoarthritis progression via inhibiting miR-155-modulated synovial macrophage M1 polarization. Rheumatology *60*, 4899–4909. https://doi.org/10.1093/rheumatology/keab018.

42. Song, M., Cui, X., Zhang, J., Li, Y., Li, J., Zang, Y., Li, Q., Yang, Q., Chen, Y., Cai, W., et al. (2022). Shenlian extract attenuates myocardial ischaemia-reperfusion injury via inhibiting M1 macrophage polarization by silencing miR-155. Pharm. Biol. *60*, 2011–2024. https://doi.org/10.1080/13880209.2022.2117828.
43. Wang, G., Liang, R., Liu, T., Wang, L., Zou, J., Liu, N., Liu, Y., Cai, X., Liu, Y., Ding, X., et al. (2019). Opposing effects of IL-1β/COX-2/PGE2 pathway loop on islets in type 2 diabetes mellitus. Endocr. J. *66*, 691–699. https://doi.org/10.1507/endocrj.EJ19-0015.
44. Nie, J., Liu, X., Lilley, B.N., Zhang, H., Pan, Y.A., Kimball, S.R., Zhang, J., Zhang, W., Wang, L., Jefferson, L.S., et al. (2013). SAD-A kinase controls islet β-cell size and function as a mediator of mTORC1 signaling. Proc. Natl. Acad. Sci. USA *110*, 13857–13862. https://doi.org/10.1073/pnas.1307698110.
45. Xu, R., Wang, K., Yao, Z., Zhang, Y., Jin, L., Pang, J., Zhou, Y., Wang, K., Liu, D., Zhang, Y., et al. (2023). BRSK2 in pancreatic β cells promotes hyperinsulinemia-coupled insulin resistance and its genetic variants are associated with human type 2 diabetes. J. Mol. Cell Biol. *15*, mjad033. https://doi.org/10.1093/jmcb/mjad033.
46. Miyazaki, J., Araki, K., Yamato, E., Ikegami, H., Asano, T., Shibasaki, Y., Oka, Y., and Yamamura, K. (1990). Establishment of a pancreatic beta cell line that retains glucose-inducible insulin secretion: special reference to expression of glucose transporter isoforms. Endocrinology *127*, 126–132. https://doi.org/10.1210/endo-127-1-126.
47. Sun, Y., Zhou, S., Shi, Y., Zhou, Y., Zhang, Y., Liu, K., Zhu, Y., and Han, X. (2020). Inhibition of miR-153, an IL-1β-responsive miRNA, prevents beta cell failure and inflammation-associated diabetes. Metabolism *111*, 154335. https://doi.org/10.1016/j.metabol.2020.154.
48. Zhu, Y., You, W., Wang, H., Li, Y., Qiao, N., Shi, Y., Zhang, C., Bleich, D., and Han, X. (2013). MicroRNA-24/MODY gene regulatory pathway mediates pancreatic β-cell dysfunction. Diabetes *62*, 3194–3206. https://doi.org/10.2337/db13-0151.
49. Li, K., Qiu, C., Sun, P., Liu, D.C., Wu, T.J., Wang, K., Zhou, Y.C., Chang, X.A., Yin, Y., Chen, F., et al. (2019). Ets1-Mediated Acetylation of FoxO1 Is Critical for Gluconeogenesis Regulation during Feed-Fast Cycles. Cell Rep. *26*, 2998–3010.e5. https://doi.org/10.1016/j.celrep.2019.02.035.
50. Fan, K.Q., Li, Y.Y., Wang, H.L., Mao, X.T., Guo, J.X., Wang, F., Huang, L.J., Li, Y.N., Ma, X.Y., Gao, Z.J., et al. (2019). Stress-Induced Metabolic Disorder in Peripheral CD4(+) T Cells Leads to Anxiety-like Behavior. Cell *179*, 864–879.e19. https://doi.org/10.1016/j.cell.2019.10.001.

STAR★METHODS

KEY RESOURCES TABLE

REAGENT or RESOURCE	SOURCE	IDENTIFIER
Antibodies		
Rabbit anti-phospho S473 AKT	Cell Signaling	Cat#4060; RRID: AB_2315049
Rabbit anti-AKT	Cell Signaling	Cat#4691; RRID: AB_915783
Rabbit anti-phospho Insulin Receptor β	Cell Signaling	Cat#3024; RRID: AB_331253
Rabbit anti-Insulin Receptorβ	Cell Signaling	Cat#3025; RRID: AB_2280448
Rabbit anti-Phospho-GSK-3β	Cell Signaling	Cat#5558; RRID: AB_10013750
Rabbit anti-GSK-3β	Cell Signaling	Cat#12456; RRID: AB_2636978
Insulin	Servicebio	Cat#GB11334-100
β-catenin	Cell Signaling	Cat#8480; RRID: AB_11127855
Rabbit anti-GAPDH	Proteintech	Cat#10494-1-AP; RRID: AB_2263076
Rabbit anti-PDX1	Abcam	Cat#Ab219207; RRID: AB_2891187
Rabbit anti-α-Tubulin	Cell Signaling	Cat#2148; RRID: AB_2288042
Goat anti-mouse IgG-HRP	Cell Signaling	Cat #7076; RRID: AB_330924
Goat anti-rabbit IgG-HRP	Cell Signaling	Cat #7074; RRID: AB_2099233
Bacterial and virus strains		
Lentivirus-GFP	This paper	N/A
Lentivirus-mmu-miR-155 sponge	This paper	N/A
Biological samples		
Human Pancreatic Islets	Tianjin First Central Hospital	N/A
Chemicals, peptides, and recombinant proteins		
Glucose	Otsuka	N/A
Insulin	Novo Nordisk	N/A
Trizol	Invitrogen	Cat#15596026
Total Exosome Isolation kit	Invitrogen	Cat#4478359
Clodronate Liposomes	LIPOSOME	Cat#CP-010-010
Hoechst 33342	Beyotime	Cat#C1022
Collagenase Type V	Sigma-Aldrich	Cat#C9263
Histopaque_-1077	Sigma-Aldrich	Cat#10771
Protease inhibitors cocktail	Roche	Cat#11687498001
Phalloidin	Yeasen	Cat#40737ES75
PKH67	Sigma-Aldrich	Cat#MINI67
Recombinant Human IL-1β	PeproTech	Cat#200-01B
Recombinant Human IFNγ	PeproTech	Cat#300-02
Recombinant Human TNFα	PeproTech	Cat#300-01A
Critical commercial assays		
Mouse Insulin ELISA	EZ assay	Cat#MS200
Insulin Radioimmunoassay	BNIBT	N/A
Lipofectamine 2000	Invitrogen	Cat#11668027
Dual-Glo Luciferase Assay Kit	Promega	Cat#E2920
BCA Protein Assays	ThermoFisher	Cat#23227
Reverse Transcription Kit	TOYOBO	Cat#FSK-101

(*Continued on next page*)

Continued

REAGENT or RESOURCE	SOURCE	IDENTIFIER
Cell Counting Kit-8 (CCK-8)	APExBIO	Cat#K1018
Exo-Fect Exosome Transfection Kit	System Biosciences	Cat#EXFT20A-1
Deposited data		
Raw and analyzed scRNA-seq data	This paper	GEO GSE232474
Experimental models: Cell lines		
Human Pancreatic Islets	Tianjin First Central Hospital	N/A
Mouse Pancreatic Islets	This paper	N/A
Mouse: L929 cell	ATCC	Cat#CCL-1
Bone Marrow-Derived Macrophage	This paper	N/A
Mouse: Min6 cell	Wang et al., 2019[43]	N/A
Rat: INS1 cell	ATCC	Cat#CM-1421
Primary islet infiltrated lymphocytes	This paper	N/A
Experimental models: Organisms/strains		
C57BL/6J Mice	GemPharmatech	N000013
db/db Mice	GemPharmatech	T002407
NOD mice	GemPharmatech	N000235
Oligonucleotides		
See Table S1 for primers	N/A	N/A
Recombinant DNA		
pMIR-REPORT	Ambion	Cat#AM5795
PDX1-wt	This paper	N/A
PDX1-mt	This paper	N/A
pCMV5-Flag	This paper	N/A
pCMV5-Flag -PDX1	This paper	N/A
pRL-SV40	Promega	Cat#E2231
Software and algorithms		
FV10-ASW	Olympus	https://lifescience.evidentscientific.com.cn/zh/downloads/detail-iframe/?0[downloads][id]=847249651
ImageJ	NIH	https://imagej.nih.gov/ij/
Pannoramic Viewer	3D HISTECH	https://www.3dhistech.com/products-and-software/software/software-downloads/
Target Scan	Whitehead Institute	http://www.targetscan.org/vert_72/
Prism	Graphpad	https://www.graphpad.com
Other		
High fat diet	Research Diets	Cat#D12492
Normal chow diet	Research Diets	Cat#D12450J
SYBR Green Mix	Vazyme	Cat#Q111-02
THUNDERBIRD Probe qPCR Mix	TOYOBO	Cat#QPS-101

RESOURCE AVAILABILITY

Lead contact

Further information and requests for resources and reagents should be directed to and will be fulfilled by the lead contact, Yunxia Zhu (zhuyx@njmu.edu.cn).

Materials availability

This study did not generate new unique reagents.

Data and code availability

- The scRNA-seq data of primary islets is available at GEO: GSE232474 and will be shared by the lead contact upon request. Accession number is listed in the key resources table.
- This paper does not report original code.
- Any additional information required to reanalyze the data reported in this paper is available from the lead contact.

EXPERIMENTAL MODEL AND STUDY PARTICIPANT DETAILS

Animals

Male C57BL6/J mice, db/db mice and NOD mice were purchased from GemPharmatech LLC. 4-week-old C57BL6/J mice were fed with a standard chow or high fat diet (HFD; 60% of kcal from fat, 20% kcal from carbohydrate and 20% of kcal from protein, Research Diets) for 4 months. All animal studies followed guidelines established by the Animal Care Committee of Nanjing Medical University, China (Permit Number: IACUC-NJMU 1404075). Mice were housed under standard specific pathogen-free conditions (24°C, 45%–55% humidity, 12 h light/dark cycle) with free access to water and food.

Primary islet isolation and cell culture

Human islets were provided from Tianjin First Central Hospital. The use of human islets was approved by the research ethics committee of Tianjin First Central Hospital (No.2018N129KY).[43] Detail information about donors was added in Table S2. Murine islets were isolated as described previously.[44] Primary islets were cultured in cultured in in medium (CMRL1066 for human islets; RPMI-1640 for murine islets) containing 10% fetal bovine serum (FBS), 100 units/ml penicillin, and 100 mg/mL streptomycin.[45] Min6 cells provided by J. I. Miyazaki (Medical School of Osaka University, Osaka, Japan) were cultured in DMEM (Invitrogen, Grand Island, NY)) with 15% FBS (Gibco, Burlington, Ontario, Canada), 100 U/ml penicillin, 100 μg/mL streptomycin, 10 mM HEPES, and 50 μM β-mercaptoethanol (Sigma, Louis, USA).[46] INS-1 cells obtained from ATCC (CM-1421) were cultured in RPMI-1640 (Invitrogen, Grand Island, NY) with 8% FBS (Gibco, Burlington, Ontario, Canada), 100 U/ml penicillin, 100 μg/mL streptomycin, 10 mM HEPES, and 50 μM β-mercaptoethanol (Sigma, Louis, USA). All the cells and primary islets were incubated at 37°C in a suitable atmosphere containing 95% O_2 and 5% CO_2.

METHOD DETAILS

Tail vein injection and abdomens aorta injection

For tail vein injection, HFD-fed male C57BL6/J mice for 4-month were injected lentivirus-miR-155 sponge (1×10^8 TU/per mouse) or GFP controls from tail vein. For abdominal aorta injection, the experiment steps are as follows: 1) Mice were fasted overnight then anesthetized with isoflurane; 2) The abdominal cavities were cut open then the abdomens aortas were exposed; 3) After injection with 100 μL antago-mir, the abdomens aortas were pressed with Q-tips for 10 min to stop bleeding. Then the abdominal cavities were washed with NS and sewed; 4) Mice were allowed 3 days postsurgical recovery. db/db mice were injected with 100 μL antago-miR-155 from the abdomens aortas as described previously.[47]

Islet-resident macrophage clearance

To clear islet-resident macrophages, clodronate liposome (LIPOSOME) was added into complete RPMI-1640 medium, the final concentration was 1 mg/mL. Primary islets were cultured in complete RPMI-1640 medium containing 1 mg/mL clodronate liposome for 24h. Macrophage clearance efficiency was confirmed by qPCR.

Metabolic characters and ELISA

Blood glucose was measured from tail vein using a Glucometer Elite monitor (Abbott, Oxon, UK). GTTs were performed by intraperitoneal (i.p.) injection of D-glucose (1 g/kg) after overnight fasting. ITTs were performed by i.p. injection of 1.2 U/kg insulin after 5 h of fasting. Mice blood samples were collected and were centrifuged at 3,000 g for 15 min to collect serum. The levels of serum insulin were measured by Insulin Elisa kit (EZ assay, Shenzhen, China).

Insulin sensitivity assays

Mice were fasted for 5 h and anesthetized by isoflurane. After anesthetization, a small piece of liver, muscle, and adipose tissues were collected avoiding hemorrhage. Then, insulin (3 U/kg) was injected via postcava and tissue samples mentioned above were collected at 3, 4, and 5 min post-injection respectively. All the samples before or after insulin injection were prepared for western blot analysis and qPCR.

Immunofluorescence staining

For pancreatic sections, mouse pancreases were collected, fixed in 4% paraformaldehyde, embedded in paraffin and cut into sections (5 μm) for further stanning overnight at 4°C with primary antibodies: β-catenin (CST, Cat#8480, 1:200), insulin (Servicebio, GB11334-100, 1:1000), and PDX1 (Abcam, ab219207, 1:1000). On the second day, sections were washed in PBS containing with 1% tween 20 (PBST), and then incubated

with second antibody (ThermoFisher, 1:500) at 37°C for 1h. Then sections were washed in PBST and stained with Hoechst 33342 (Beyotime, 1:8000) before imaging by confocal microscopy (Olympus). For cell lines, Min6 cells were stained with phalloidine (Yeasen, Shanghai, China) according to the manufacturer's protocol.

Bone marrow-derived macrophage isolation

8-10 weeks C57BL6/J mice were sacrificed for bone marrow-derived macrophages (BMDM) isolation. BMDM was collected and treated as described previously.[23] The unpolarized M0 macrophages and differentiated M1 or M2 macrophages were cultured in RPMI-1640 medium containing 10% FBS (exosome-free), 100 units/ml penicillin, and 100 mg/mL streptomycin for 48h to collect culture media for further exosomes extraction as described previously.[21]

BMDM-derived exosomes isolation

Collected culture media were centrifuged at 2000 rpm for 5 min to pellets cells and then at 10,000 g for 20 min to discard dead cells and cell debris. Exosomes were then isolated using Total Exosome Isolation kit (Invitrogen, Grand Island, NY) and were identified by western blot and TEM as reported.[20]

Exosomes transfection

Isolated M1 macrophage-derived exosomes (M1-exos) (25μg) were transfected with 10 p.m. anti-miR-155-5p using the Exo-Fect Exosome Transfection Kit (System Biosciences, Palo Alto, CA, USA) and added to exosome-free medium for Min6 cells to culture for 48h.

Fluorescence labeling of exosomes

Exosomes were labeled with PKH67 (Sigma, Louis, USA) for 1 h and then washed three times with PBS. PKH67-labeled exosomes were resuspended in RPMI-1640 and incubated with cultured Min6 cells. After incubation for 24 h, Min6 cytoskeleton was stained with Phalloidin (Yeasen, Shanghai, China) while nucleus was stained with Hoechst 33342 (Beyotime, Shanghai, China). Macrophages were examined by confocal microscopy (FV1200; Olympus).

GSIS, KSIS and islet perfusion assay

Min6 cells and mouse/human islets or INS1 cells were transfected with miR-155 mimics or anti-miR-155 for 48h were subjected to glucose-stimulated insulin secretion (GSIS) or potassium-stimulated insulin secretion (KSIS) assay.[48] Insulin content was extracted using acid-ethanol. For islet perfusion, after equilibrating overnight, 100 islets per group were incubated 1 h at 37°C in Krebs-Ringer buffer (KRB) with 0 mM glucose, then collected in a syringe filter (Millex-GP, Millipore) and perfused with 37°C KRB containing 0 mM glucose for 25 min at 125 μL/min flow rate, then followed by 20 mM glucose for 15 min. Insulin levels were measured by radioimmunoassay.[48]

Western blot analysis

Western blotting was performed as described previously[48] using primary antibodies against P-AKT (CST, Cat#4060, 1:2000); AKT (CST, Cat#4691, 1:1000); P-INSR (CST, Cat#3024, 1:1000); INSR (CST, Cat#3025, 1:1000); P-GSK3β (CST, Cat#5558, 1:1000); GSK3β (CST, Cat#12456, 1:1000); GAPDH (Proteinech, Cat No. 10494-1-AP, 1:10000); PDX1 (Abcam, ab219207, 1:1000); α-tubulin (CST, Cat#2148, 1:4000). Secondary antibodies were goat anti-rabbit IgG-HRP (CST, Cat #7074, 1:4000) and anti-mouse IgG-HRP (CST, Cat #7076, 1:4000). Stripes intensity was measured by ImageJ.

RNA extraction and qPCR

Total RNA was extracted with TRIzol reagent (Invitrogen, Grand Island, NY). The reverse transcriptions of miRNA and mRNA were performed according to the instructions of TOYOBO and Vazyme respectively.[21] Quantitative RT-PCR were performed by using the THUNDERBIRD probe qPCR Mix (TOYOBO) for miR-155-5p, and SYBR Green qPCR Master Mix for mRNA on Roche Lightcycle480 II Sequence Detection System (Roche Diagnostics). U6 and β-actin were used as normalizers for miRNAs and mRNAs, respectively. TaqMan probes for mmu-miR-155-5p (002571) and has-miR-155-5p (000479) detection were purchased from ThermoFisher. Primer sequences for qPCR were listed in Table S1.

Plasmid construction and luciferase assay

Mmu-miR-155 binding sites of 3′UTR of PDX1 and relative mutant nucleotide sequences were synthesized and inserted into pMIR-REPORT Luciferase miRNA Expression Reporter Vector (Ambion, Foster City, CA).[49] pRL-SV40 carried Renilla luciferase was used as internal control. Min6 cells were transfected with luciferase reporter plasmids and pRL-SV40 as well as mmu-miR-155 mimics or negative control using Lipofectamine 2000 (Invitrogen, Grand Island, NY) according to the manufacturer's instructions. After 48h transfection, luciferase activities were measured with a dual-luciferase reporter assay system (Promega, Madison, WI) and normalized to Renilla activity expressed with the pRL-SV40 plasmid.

Single-cell RNA sequencing (scRNA-seq)

Freshly isolated islets were cultured in culture media (5.5 mM glucose) for 4 h and then processed to obtain dispersed single cells. Cells was then examined by cell counter (Ruiyu Biotech, Shanghai, China) to ensure more than 90% viability. 10 x Genomics ChromiumTM platform was used to prepare scRNA-seq library. The resulting libraries were sequenced on an Illumina Hiseq PE150 platform. The data cleaning, normalization and scaling were handled by Cell Ranger algorithm (Novogene, Beijing, China).[50] Principal component analysis was used to reduce dimension and all cells were projected onto a two-dimensional map by means of t-stochastic neighbor embedding (t-SNE). Cell types were then clustered through a k-means-based approach and visualized by Loupe-Cell-Browser-2.0.0 (Novogene). Marker genes of each cell cluster were outputted to define the cell types. scRNA sequencing data are available in GEO GSE232474.

QUANTIFICATION AND STATISTICAL ANALYSIS

In vitro experiments were repeated at least three times and *in vivo* assay were repeated two times, with the number of per condition or mice included in each group in each experiment indicated. The areas of islets and pancreas were calculated using Slide Viewer software. Comparisons were performed using the Student's t test between two groups or ANOVA in multiple groups. Results are presented as mean ± SEM. $p < 0.05$ is considered statistically significant.